IGBT-Gating Failure Effect on a Fault-Tolerant Predictive Current Controlled 5-Phase Induction Motor Drive

H. Guzman, F. Barrero, *Senior Member, IEEE*, M. J. Duran

***Abstract*—Multiphase machine drives are gaining importance in high reliability applications due to their fault-tolerance capability and their ability to cope with the post-fault operation without any extra electronic components. Predictive current controllers have been recently proposed for managing post-fault operation of these drives when an open phase fault is considered. However, the faulty situation assumes zero stator current while free-wheeling diodes can continue conducting in a non-controlled mode. This work analyses the post-fault operation of the five-phase drive when the free-wheeling diodes of the faulty phase are still conducting. Experimental results are provided using a conventional IGBT-based multiphase power converter to quantify the effect of the free-wheeling diodes, when an IGBT-gating fault occurs, on the model-based predictive current controlled drive.**

***Index Terms*—Multiphase drives, Post-fault operation, Fault-tolerance, IGBT gating fault, Free-wheeling diodes, Predictive controllers.**

I. Introduction

Fault-tolerance is one of the most attractive features of multiphase drives. The ability of multiphase machines to continue working as long as three healthy phases exist have made them attractive for applications where post-fault operation is a main concern for economical/safety reasons [1].

Previous work has been done regarding the fault-tolerance of multiphase drives, including the electrical drive design [2], converter topologies [3], post-fault machine behavior [4], modeling [5], and control strategies [6, 7]. More recently, predictive control methods have been applied to multiphase drives, showing their interest in pre- and post-fault operation of the system [8]. Nevertheless, all this body of knowledge is solely related to open-phase faults, while the effect of the free-wheeling conduction of the diodes included in standard IGBT power stacks has only been mentioned in [2], but it has not been addressed yet. Voltage source inverter (VSI) faults can be roughly divided in two groups; open-phase (OPF) and IGBT gating faults (IGBT-GF) [2]. In the first case the current cannot flow through the faulty phase while in the latter, a non-controlled current still flows through the diodes after the IGBT gating fault appears, unless the faulty phase is disconnected from the electrical machine using additional electric protection components [9]. This letter extends the analysis in [8], where a fault-tolerant finite-control-set model-based predictive (FCS-MPC) current control system is presented, quantifying the effect of the free-wheeling diodes of the faulty phase on the controlled drive (IGBT-GF fault type). The paper is organized as follows. Section II summarizes the mathematical model of the 5-phase induction motor drive and details the operation states after the fault occurrence. The post-fault control is presented in section III and the OPF and IGBT-GF post-fault operation is experimentally tested and compared in Section IV. Conclusions are finally summarized in the last section.

Manuscript received November 8, 2013; revised February 27, 2014; accepted May 15, 2014.

This work was supported by the Spanish Government (National Research, Development and Innovation Plan, under references DPI2011-25396 and DPI2009-07955, and Junta de Andalucía 2010 research program, under reference TEP-5791) and Andalucía Tech International Campus of Excellence.

H. Guzman and M.J. Duran are with the Electrical Engineering Department, University of Málaga, C/ Doctor Ortiz Ramos s/n, 29071 Spain, (email: hugguzjim@uma.es, mjduran@uma.es).

F. Barrero is with the Electronic Engineering Department, University of Seville, Avda. de los Descubrimientos s/n, 41092 Spain, (email: fbarrero@etsi.us.es).

II. 5-Phase Converter in IGBT-GF Operation Mode

Power converters are commonly based on IGBT stacks due to their ease of use and wide variety of power ranges. A converter with the ability to disconnect the whole power converter is not interesting in a multiphase drive due to their null fault-tolerant capability. Instead, phase-leg independent power converters are preferred, where a fault in a phase can be managed while the machine continues operating. These power converters require also additional components if the faulty phase must be disconnected from the electrical machine when the fault appears. Otherwise, the switching sequence on the faulty phase stops, leaving the free-wheeling diodes connected to the machine in a non-controlled mode of operation. In the latter case, the IGBT-GF post-fault operation mode is achieved and the stator current of the faulty phase cannot be assumed as zero (Fig. 1, switch S_w in ON state). In what follows, it will be assumed without any lack of generality that phase "*a*" is the faulty phase. Then, its free-wheeling diodes, D_1 and D_2, conduct current to the positive (*P*) or the negative (*N*) rail of the converter when they are forward-biased (1)-(2):

$$D_1 - ON: \; V_{D1} = v_{as} + V_{CM} - 0.5 \cdot V_{DC} \geq V_\gamma \tag{1}$$

$$D_2 - ON: \; V_{D2} = v_{as} + V_{CM} + 0.5 \cdot V_{DC} \leq -V_\gamma$$

$$V_{CM} = V_{sN} - \frac{V_{DC}}{2} = \frac{1}{5} \cdot (V_{aN} + V_{bN} + V_{cN} + V_{dN} + V_{eN}) - \frac{V_{DC}}{2} \tag{2}$$

where v_{as} is the faulty phase voltage, V_γ is the diode forward conduction voltage, and V_{CM} is the common-mode voltage (CMV) that relates the motor neutral voltage *s* to the DC-link mid-point *O*.

This article has been accepted for publication in a future issue of this journal, but has not been fully edited. Content may change prior to final publication. Citation information: DOI 10.1109/TIE.2014.2331019, IEEE Transactions on Industrial Electronics

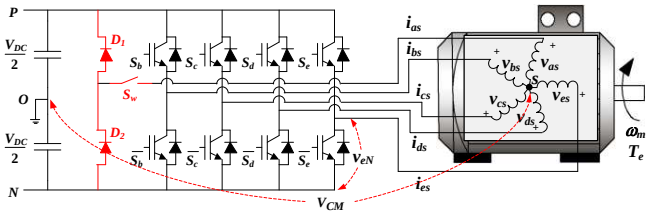

Fig. 1. Two-level five-phase IGBT-based voltage source inverter under IGBT-GF (S_w in ON state) or OPF (S_w in OFF state) modes.

The voltages of the remaining healthy phases (V_{iN}, i={b,c,d,e}) depend on the switching states S_i in the form V_{iN}=S_i·V_{DC}, being S_i=0 if the lower power switch is ON and the upper is OFF and S_i=1 if the opposite occurs. If none of the free-wheeling diodes are conducting, the drive is functioning in OPF mode and the phase voltage matrix is given by (3) and (4), according to [8]. Notice the absence of phase "*a*" voltage and the inclusion of the $BEMF_a$ (back-emf of the faulty phase) and the factor 1/4 instead of 1/5, due to appearance of the $BEMF_a$ term on the voltage equilibrium equations [8]. The last row in (3) expresses the voltage between the machine neutral point and the inverter negative rail, providing the CMV in (4). Phase voltages do not have a fixed value for a certain switching state S_i, as it occurs in pre-fault condition. On the contrary, phase voltages depend on $BEMF_a$ in the OPF mode of operation, and consequently on the operating point of the drive.

$$\begin{bmatrix} v_{bs} \\ v_{cs} \\ v_{ds} \\ v_{es} \\ V_{sN} \end{bmatrix} = \frac{1}{4} \begin{bmatrix} 3 & -1 & -1 & -1 & -1 \\ -1 & 3 & -1 & -1 & -1 \\ -1 & -1 & 3 & -1 & -1 \\ -1 & -1 & -1 & 3 & -1 \\ 1 & 1 & 1 & 1 & 1 \end{bmatrix} \begin{bmatrix} V_{bN} \\ V_{cN} \\ V_{dN} \\ V_{eN} \\ BEMF_a \end{bmatrix} \tag{3}$$

$$V_{CM} = \frac{1}{4} BEMF_a + \frac{1}{4}\left(V_{bN} + V_{cN} + V_{dN} + V_{eN}\right) - \frac{V_{DC}}{2} \tag{4}$$

However, if any of the conditions in (1) are satisfied, which depends on the $BEMF_a$ value, the drive enters the IGBT-GF mode of operation where D_1 or D_2 ON state must also be considered. In this case, i_{as} is not null, as experimentally verified in [9], although the sum of the phase voltages is zero:

$$0 = v_{as} + v_{bs} + v_{cs} + v_{ds} + v_{es} \tag{5}$$

Considering (5), the resulting phase voltage matrix and V_{sN} value are obtained as follows:

$$\begin{bmatrix} V_{as} \\ V_{bs} \\ V_{cs} \\ V_{ds} \\ V_{es} \\ V_{sN} \end{bmatrix} = \frac{1}{5} \begin{bmatrix} 4 & -1 & -1 & -1 & -1 & 1 \\ -1 & 4 & -1 & -1 & -1 & 1 \\ -1 & -1 & 4 & -1 & -1 & 1 \\ -1 & -1 & -1 & 4 & -1 & 1 \\ -1 & -1 & -1 & -1 & 4 & 1 \\ 1 & 1 & 1 & 1 & 1 & -1 \end{bmatrix} \begin{bmatrix} V_{aN} \\ V_{bN} \\ V_{cN} \\ V_{dN} \\ V_{eN} \\ 0 \end{bmatrix} \tag{6}$$

$$V_{sN} = \frac{1}{5}\left(V_{aN} + V_{bN} + V_{cN} + V_{dN} + V_{eN}\right) \tag{7}$$

Although the switching state depends on the four healthy phases in the IGBT-GF mode of operation, notice that the non-controlled phase is connected to the positive rail of the converter (P) if D_1 is ON or to the negative rail (N) if D_2 is ON. Then, the stator voltage of the faulty phase is fixed when any of the free-wheeling diodes is ON, and a degree of freedom is lost. In this case, the common-mode voltage of the machine can be estimated using (2). Moreover, notice that the non-controlled current will affect the machines stator neutral voltage and the electrical drive will be constantly changing its configuration. Fig. 2 shows available voltage vectors in OPF mode of operation as stated in [8] (Fig. 2a), and available voltage vectors that appear when any of the free-wheeling diodes is ON (Fig. 2b). Two different sets of available space vectors appear in α-β-x-y planes in Fig. 2b, depending on the conducting free-wheeling diode; black lines represent the case when D_1 is ON and D_2 is OFF, while red colored lines depict the available vectors when D_1 is OFF and D_2 is ON. Then, three different sets of space vectors appear in a single period during IGBT-GF fault operation mode, those corresponding to the OPF operation mode where D_1 and D_2 are OFF (Fig. 2a) plus those where one free-wheeling diode is ON (Fig. 2b). This is of great importance when predictive methods are used due to the imperative need of an accurate plant model. Thus, it is necessary to verify and quantify the effect of an IGBT-GF fault on the proposed open-phase fault-tolerant FCS-MPC, as it is stated in [8].

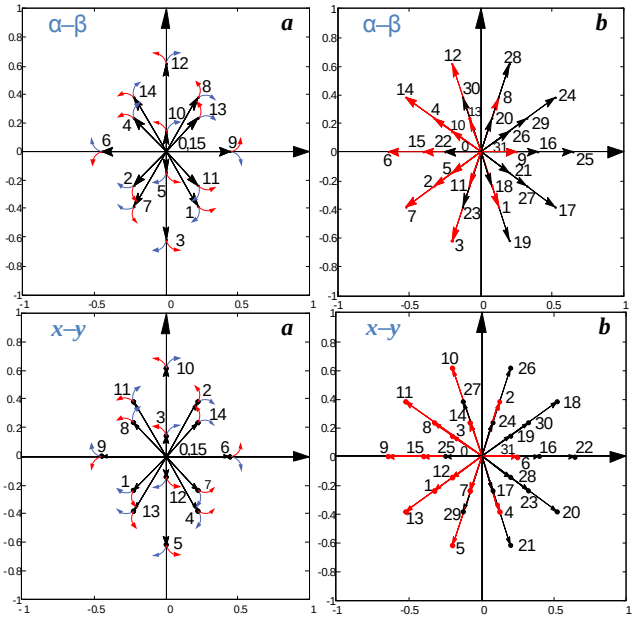

Fig. 2. Available voltage vectors in the α-β (upper plots) and x-y (lower plots) planes. (a) OPF mode of operation. (b) IGBT-GF mode of operation, being D_1 ON and D_2 OFF (black ink) or D_1 OFF and D_2 ON (red ink).

III. Post-Fault Control

The post-fault control consists of an outer speed control loop that provides the □-□ reference currents to an inner FCS-MPC current control (Fig. 3). The y current reference is set according to a predefined criterion. Minimum copper losses (MCL) operation is achieved with □ □ □, but the unequal magnitude of phase currents limits the maximum achievable □-□ currents to □□□□□ of the nominal pre-fault current [8]. On the other hand, minimum derating (MD) is achieved by setting □ □ □□□□□□□□. In this case all phase currents have equal magnitudes and this symmetry elevates the maximum achievable □-□ currents to □□□□□ of the nominal pre-fault current [8]. As a result, the maximum achievable torque is higher with MD than with MCL criterion. Regardless of the selected control criteria, the loss of phase "*a*" results in a fixed

This article has been accepted for publication in a future issue of this journal, but has not been fully edited. Content may change prior to final publication. Citation information: DOI 10.1109/TIE.2014.2331019, IEEE Transactions on Industrial Electronics

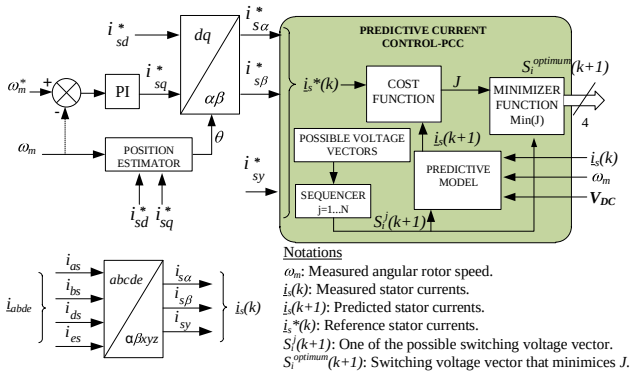

Fig. 3. Implemented post-fault control with an inner finite-control set model-based predictive current control scheme and an outer speed control loop.

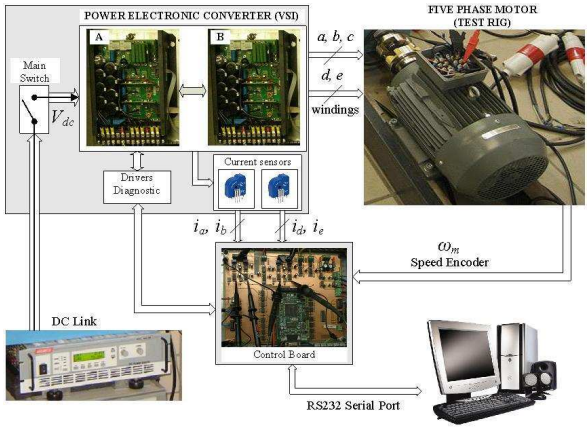

Fig. 4. Experimental test bench formed by two conventional 3-phase VSIs, a five-phase induction machine and a TI F28335 based electronic control board.

relation between the □ and □ components (□□ □ □□□). Considering the □, □ and *y* current references as inputs (Fig. 3), the inner FCS-MPC current control uses a model of the system (in an open-phase fault) to predict the future currents of the drive and selects the switching state that minimizes a certain cost function, which in this case only aims to minimize the current error [8]. The optimum switching state is applied during the whole sampling period avoiding the modulation stage.

IV. OPF VS IGBT-GF POST-FAULT OPERATION MODES

The effect of an IGBT-GF fault is now evaluated in the open-phase fault-tolerant control. The faulty phase diodes are not included in the predictive model, allowing to estimate the effect of the non-controlled current [9], in the proposed control and compare its performance with OPF operation. Then, the same experimental setup as in [8], Fig. 4, has been used, with a maximum switching frequency of 10 kHz and a DC-link voltage of 300 V. The stator current reference in *d*-axis is set to 0.57 A, while in *q*-axis is set to either 2.43 A (pre-fault), 1.6 A (post-fault with MCL) and 1.71 A (post-fault with MD).

First, a post-fault speed response test is performed (Fig. 5). The speed (first and third plots) and *q* current component (second and fourth plots) are compared implementing the MCL (Fig. 5a) and the MD (Fig. 5b) methods, for OPF and IGBT-GF fault states. A speed change from 0 to 500 rpm is done at about t = 0.1 s, then a constant load torque (T_L) of approximately 28% the nominal torque (T_n) is demanded by means of a mechanically coupled DC-machine. It can be noted that the effect of free-wheeling diodes is mostly neglectable since the electrical drive is working below its maximum post-fault rating. This situation differs if the drive is operated close to the maximum ratings as it will be shown next.

A second test is performed to observe the pre- and post-fault transition during OPF and IGBT-GF faults, implementing the MCL (Fig. 6a) and MD (Fig. 6b) criteria, with a speed reference of 500 rpm. The OPF and IGBT-GF faults are generated in phase "*a*" at t = 0.2 s, using the power relay to open the faulty phase or interrupting the IGBT's switching scheme, respectively. The control system is reconfigured instantaneously after the fault occurrence. Consequently, the transient state during fault detection is not considered. Two different working points are analyzed for each control method, maintaining the demanded load torque within the post-fault ratings of each criterion, (T_L = 0.56·T_n) for MCL and (T_L = 0.64·T_n) for MD [8]. Notice that for low load torque conditions (first and third plots), the effect of the

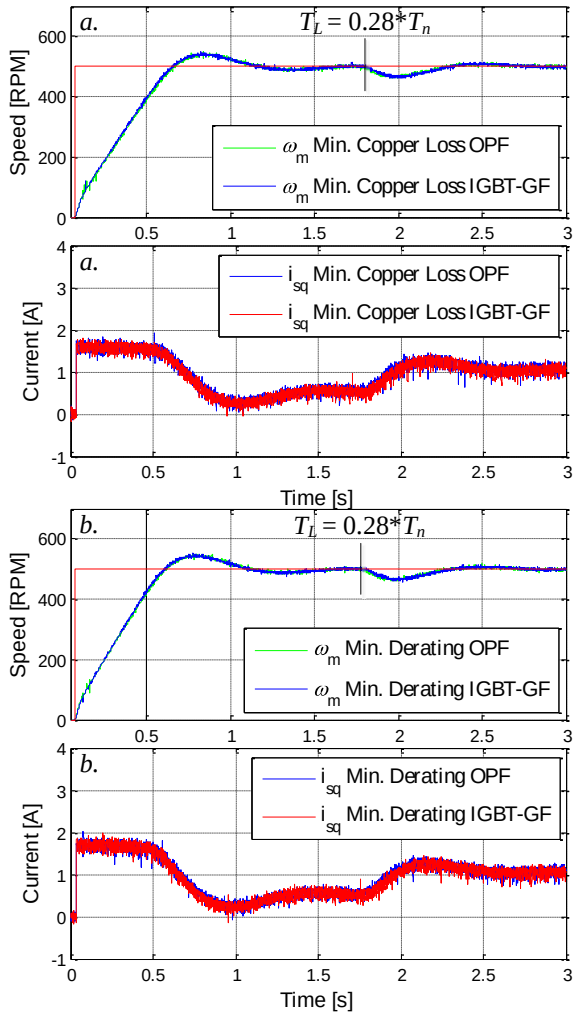

Fig. 5. Post-fault speed response tests during OPF or IGBT-GF faults. First, a step in the reference speed from 0 to 500 rpm is applied at about t=0.1 s. Then, a load torque (28% of the rated torque) is imposed at t=1.8 s. Speed (upper Fig. 5a and 5b plots) and *q* current response (lower Fig. 5a and 5b plots) for the MCL (a) and MD (b) criteria.

This article has been accepted for publication in a future issue of this journal, but has not been fully edited. Content may change prior to final publication. Citation information: DOI 10.1109/TIE.2014.2331019, IEEE Transactions on Industrial Electronics

non-controlled current can be barely observed and the control performance is similar for OPF and IGBT-GF faults. However, when the drive is operated close to the maximum working capability for each control criteria, the speed reference is not achieved after the fault occurrence, maintaining a maximum speed of approximately 490 rpm (second and fourth plots) with an increment in the rms currents of 1% in the healthy phases. This deterioration in the performance is further increased when the fault detection delay is considered (Fig. 7), where a fault detection delay of 40 ms is emulated and the minimum derating criterion is implemented. Observe that the delay in the post-fault control of the electrical drive results in an error of the controller performance (achievable post-fault speed was 480 rpm with a reference speed of 500 rpm). As a result, the non-inclusion of the effect of the IGBT's free-wheeling diodes in the predictive modeling of the fault-tolerant FCS-MPC controller outcomes in a deterioration of the post-fault electrical drive ratings, mainly due to the difference between the considered and the applied voltage vectors (Fig. 2). This deterioration increases with higher values of the load torque or fault detection delay, but the obtained experimental results state that it is limited to a small percentage of the overall performance. Then, it can be considered as an external controller perturbation, which reduces the cost of the required power converter avoiding additional electric components to manage the fault.

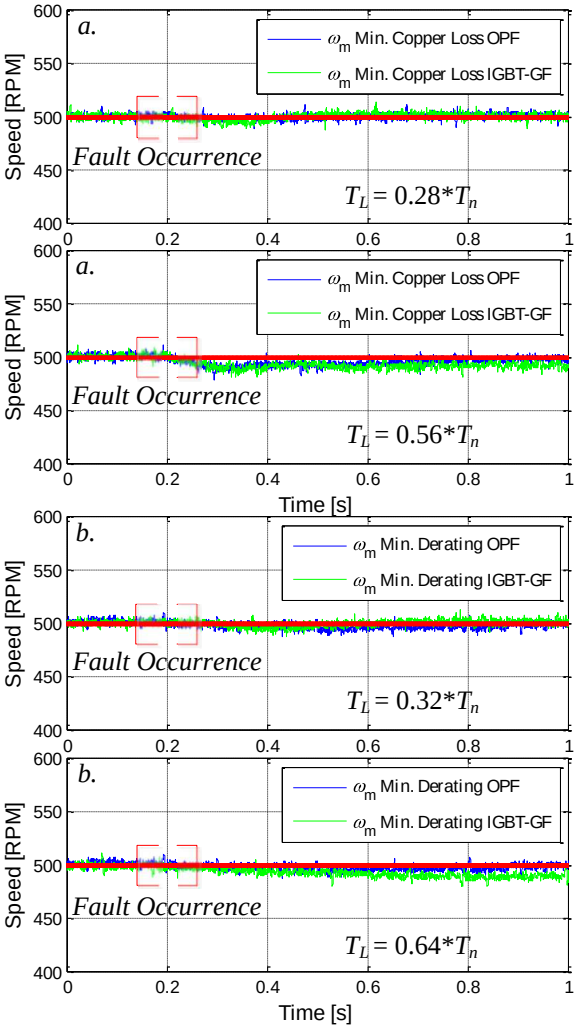

Fig. 6. Pre- and post-fault system performance when an OPF or IGBT-GF fault appears. Speed response with different load torque conditions (T_L) is considered. The fault appears at t = 0.2 s. Post-fault operation is managed using the MCL (a) and MD (b) criteria with a reference speed of 500 rpm.

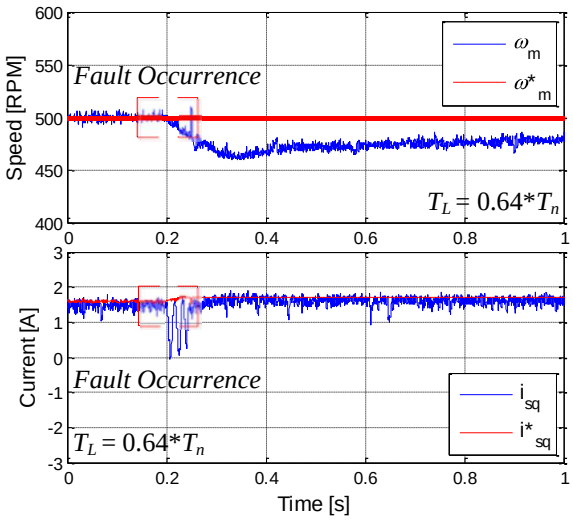

Fig. 7. Fault detection delay effect. Speed (left plot) and q-current (right plot) are shown when a fault occurs at t=0.2 s implementing the minimum derating method during post-fault operation with a constant load torque of T_L, before and after the fault occurrence. The fault is detected 40 ms after its occurrence.

V. Conclusion

In the event of a phase fault condition in a multiphase VSI, two main situations can be found; open-phase and IGBT gating failure states. Open-phase situation requires additional electric components in the VSI to manage the fault which increases the cost and complexity of the power converter. The IGBT gating fault case reduces this extra cost and complexity, introducing an additional non-controlled oscillation in the stator neutral voltage. This paper analyzes from theoretical and experimental perspectives the effects of this oscillation due to a non-controlled stator phase. The control performance of the entire system in post-fault situation is studied when the free-wheeling diodes are considered, concluding that not using extra components in the power converter increases the deterioration of the faulty multiphase drive when it is operated at its maximum post-fault ratings and some detection delay is considered. However, the degradation in the control performance is limited and can be considered as an external perturbation of the controller. The free-wheeling diode stator currents slightly reduce the torque production and increase copper losses, maintaining the basic features of the post-fault operation controlled system.

References

[1] E. Levi, R. Bojoi, F. Profumo, H. Toliyat, S. Williamson, "Multiphase induction motor drives–a technology status review," *IET Electric Power Applications*, vol. 1, no. 4, pp. 489–516, 2007.

[2] L. Lillo, L. Empringham, P.W. Wheeler, S. Khwan-On, C. Gerada, M.N. Othman, X. Huang, "Multiphase Power Converter Drive for Fault-Tolerant Machine Development in Aerospace Applications," *IEEE Trans. on Ind. Electron.*, vol. 57, no. 2, pp. 575-583, 2010.

[3] N. Bianchi, E. Fornasiero, S. Bolognani, "Performance of Five-Phase Motor Drive Under Post-Fault Operations," *Electric Power Components and Systems*, vol. 39, no. 12, pp. 1302-1314, 2011.
[4] L. Alberti, N. Bianchi, "Experimental Tests of Dual Three-Phase Induction Motor Under Faulty Operating Condition," *IEEE Trans. on Ind. Electron.*, vol. 59, no. 5, pp. 2041-2048, 2012.
[5] R. Kianinezhad, B. Nahid-Mobarakeh, L. Baghli, F. Betin, GA. Capolino, "Modeling and Control of Six-Phase Symmetrical Induction Machine Under Fault Condition Due to Open Phase," *IEEE Trans. on Ind. Electron.*, vol. 55, no. 5, pp. 1966-1977, 2008.
[6] S. Dwari. L. Parsa, "Fault–tolerant control of five–phase permanent–magnet motors with trapezoidal back EMF," *IEEE Trans. on Ind. Electron.*, vol. 58, no. 2, pp. 476-485, 2011.
[7] N. Bianchi, S. Bolognani, M.D. Pré, "Strategies for the Fault-Tolerant Current Control of a Five-Phase Permanent-Magnet Motor," *IEEE Trans. on Ind. App.*, vol. 43, no. 4, pp. 960-970, 2007.
[8] H. Guzman, M.J. Duran, F. Barrero, B. Bogado, S. Toral, "Speed Control of Five-Phase Induction Motors with Integrated Open-Phase Fault Operation using Model-Based Predictive Current Control Techniques," *IEEE Trans. on Ind. Electron.*, vol. 61, no. 9, pp. 4474-4484, 2014.
[9] H. Guzman, M.J. Durán, J.A. Riveros, F. Barrero, "Modeling of a Five-Phase Induction Motor Drive with a Faulty Phase," *15th International Power Electronics and Motion Control Conference (EPE-PEMC 2012)*, Novi Sad, Republic of Serbia.

Hugo Guzman received the B.Eng. degree in Electronic Engineering from the Pontificia Universidad Javeriana, Bogotá-Colombia, in 2009 and MSc. Degree from the University of Seville, Spain in 2011. Mr. Guzmán joined the Electronic Engineering Department of the University of Seville in 2007 working as a research assistant and from 2010 to 2012 worked toward his PhD degree. He is currently a researcher at the University of Málaga, Electrical Engineering Department, funded by an Andalucía Tech scholarship (2013).

Federico Barrero (M 04; SM 05) received the MSc and PhD degrees in Electrical and Electronic Engineering from the University of Seville, Spain, in 1992 and 1998, respectively. In 1992, he joined the Electronic Engineering Department at the University of Seville, where he is currently an Associate Professor. He received the Best Paper Awards from the IEEE Transactions on Industrial Electronics for 2009 and from the IET Electric Power Applications for 2010-2011.

Mario J. Duran was born in Málaga, Spain, in 1975. He received the M.Sc. and Ph.D. degrees in Electrical Engineering from the University of Málaga Spain, in 1999 and 2003, respectively. He is currently an Associate Professor with the Department of Electrical Engineering at the University of Málaga. His research interests include modeling and control of multiphase drives and renewable energies conversion systems.